Detecting Start of Combustion using Knock Sensor Signals

Examensarbete utfört i Fordonssystem
vid Tekniska Högskolan i Linköping
av

Mats Järgenstedt

Reg nr: LiTH-ISY-EX-3035

Detecting Start of Combustion using Knock Sensor Signals

Examensarbete utfört i Fordonssystem
vid Tekniska Högskolan i Linköping
av

Mats Järgenstedt

Reg nr: LiTH-ISY-EX-3035

Supervisor: **Magnus Pettersson**

Examiner: **Lars Eriksson**

Linköping, September 25, 2000.

Avdelning, Institution
Division, Department

Vehicular Systems
Dept. of Electrical Engineering

Datum:
Date:

2000-09-25

Språk
Language

☐ Svenska / Swedish
☒ Engelska / English
☐ ______

Rapporttyp
Report category

☐ Licentiatavhandling
☒ Examensarbete
☐ C-uppsats
☐ D-uppsats
☐ Övrig rapport
☐ ______

ISBN

ISRN

Serietitel och serienummer
Title of series, numbering

ISSN

LiTH-ISY-EX-3035

URL för elektronisk version

http://www.fs.isy.liu.se/

Titel: Detektering av förbränningsstart med hjälp av knacksensor
Title: Detecting Start of Combustion using Knock Sensor Signals

Författare: Mats Järgenstedt
Author:

Sammanfattning
Abstract

Fördelarna med att veta förbränningsstarten i en direktinsprutad dieselmotor är flera. Exempel är förmågan att optimera bränsleförbrukningen gentemot utsläppsnivån och ökade möjligheter att diagnostisera insprutningsutrustningen. Återkoppling av förbränningsstarten möjliggör dessutom användandet av billigare elektronik och mekanik. Dagens motorstyrsystem använder sig i bästa fall av återkoppling av insprutningen. Eftersom det är förbränningen som ger upphov till kraften och utsläppen och eftersom fördröjningen mellan insprutnings- och förbränningsstart varierar, så vore det mycket bättre att kontrollera förbränningsstarten.

En ny teknik för detektion av förbränningsstarten som bygger på analys av knacksignaler beskrivs här. Metoden baseras på mätta signaler från billiga och mycket använda knacksensorer. Signalerna bandpassfiltreras, den resulterande signalens envelopp räknas ut och slutligen jämförs enveloppens värden med en tröskelnivå. Denna tröskelnivå beskrivs i procent av enveloppens maximala värde och förbränningsstarten sägs äga rum när detta tröskelvärde passeras.

Standardavvikelsen för fördröjningen mellan mätt insprutningsstart och detekterad förbränningsstart är mindre än 0.1 vevvinkelgrad i samtliga experiment. Metoden kan detektera förbränningsstarten i realtid och möjliggör därmed sluten styrning av förbränningsstarten. Denna styrning gör det möjligt för motorstyrsystemet att korrigera för ändringar i lufttemperaturen, fuktinnehållet, bränslekvaliteten och för fel i insprutarnas inställningar. Därigenom kan olikheter mellan individuella cylindrar minimeras.

Nyckelord
Keywords

knack, knock, SOI, SOC, diesel, DI

Abstract

The benefits from knowing the start of combustion (SOC) in a direct injection diesel engine are numerous. Examples are the ability to optimize the fuel consumption versus the emissions and an increase in diagnostic features of the injection equipment. By using feedback from SOC it would also be possible to use less expensive electronics and mechanics. Engine management systems of today utilize, at very best, closed loop control of the start of injection with good precision. However, it is the combustion that produces power and emissions and since the delay between the start of injection and the start of combustion varies with several factors, it would be much better to control SOC.

A new technique for detecting start of combustion by knock signal evaluation is described. The method is based on measurements from widely used and inexpensive knock sensors which measure a knock signal. The signal is thereafter band pass filtered, the envelope of the resulting signal is calculated and finally compared to a threshold expressed as a percentage of the maximum value of the envelope. SOC is said to occur when the envelope exceeds the threshold.

The standard deviation of the delay between the measured start of injection and the detected start of combustion in all experiments is less than 0.1 crank angle degree. The method detects SOC in real time and makes it possible to control SOC with closed loop strategy. The closed loop control strategy makes it possible for the engine control system to correct for changes in for example the air temperature, moisture content, fuel quality and for errors in the accuracy of the injectors. Thereby the differences between individual cylinders and different engines can be minimized.

Contents

Explanations

EGR Exhaust Gas Recirculation. By recirculating exhaust gases the percentage of oxygen is lowered.

TDC Top Dead Center. The highest position of the piston. The corresponding crank angle is often set to the relative crank angle 0°.

BDC Bottom Dead Center. The lowest position of the piston. Corresponding crank angle is 180°.

SI Spark Ignition.

SOI Start Of Injection.

SOC Start Of Combustion.

PDE Pumpe-Düse-Einheit [German]
Unit pump injection.

Warm Side The exhaust gas side of the engine.

Cold side The inlet air side of the engine.

α SOI expressed in crank angles counted from TDC. Almost always a negative number.

HC Hydrocarbons

NOx Nitric oxides

r.p.m. Revolutions per minute

EVC Exhaust valves close

EVO Exhaust valves open

IVC Inlet valves close

IVO Inlet valves open

Chapter 1

Introduction

The emissions from and the fuel efficiency of a diesel engine depend directly on the start of combustion (SOC). Due to high compression and thereby auto ignition, SOC occurs shortly after the diesel is injected. On one hand the combustion must not occur too early because of the increased NOx production in that case. One the other hand SOC must not be too late due to decreased fuel efficiency. These demands are contradicting and it is therefore of importance to know SOC in order to allow an optimization. The future emission legislation will require high precision for the opening and closing of the injectors in direct injection diesel engines. The systems of today depend on small mechanical tolerances and expensive electronics or at the very best on measurements of the start of injection (SOI). The measurements make closed loop control of SOI possible. The delay between SOI and SOC however changes with for example the temperature of air, fuel and engine, the atmospheric humidity, the fuel cetane number and the EGR (exhaust gas recirculation) content so it would be much more informative to measure SOC. This could be done if pressure or ion currents in the cylinder is measured [2, 3], but neither of these approaches are feasible in production diesel engines today.

The novel idea of this study is to estimate SOC by evaluating a measured knock, i.e. accelerometer, signal. For spark ignited (SI) engines knock is the harmful phenomenon of auto ignition. For such engines knock is thoroughly studied and a number of strategies for the detection is developed [4, 7]. In diesel engines however, auto ignition is the normal working principle and the instant when it occurs is important. If this instant could be detected it would enable closed loop control of SOC by means of inexpensive knock sensors and existing control systems. By using closed instead of open loop control, it is possible to disregard the different dependences described above and the individual scattering in the injector equipment and thereby lower the fuel consumption due to the better optimization of SOC. It is also possible to use less expensive mechanics and electronics due to the lowered demands upon the equipment and even to diagnose the injector equipment and thereby enable flexible service intervals. Errors that can be detected are for example if an injector is stuck close or open or if the timing of an injector is to early or to late. It could perhaps even be possible to diagnose the timings of the valves and to diagnose the quality of the fuel by calculating the ignition delay if SOI is measured.

Chapter 2
Experimental Equipment

This chapter describes and shows the equipment used in the experiments. Essential for the potential of knock evaluation is the sensor location. This problem is treated in Section 2.2

2.1 Experimental Engines

Two different engines are used. Both engines are four stroke diesel engines with direct injection systems. The injection system used is the Bosch unit injector and to simplify it greatly, a needle is lifted in order to open the holes in the injector. This enables the diesel to be injected under a pressure of approximately 1200 bar. It is possible to measure SOI with good precision in this system and thereby utilize closed loop control of the needle lift. This makes the system very accurate and predictable with respect to SOI [1].

Operating Principle of a Four Stroke Diesel Engine

Unlike the Otto engine, the diesel engine does not demand a sparking plug. The work cycle is divided into four strokes. The first stroke begins with the closing of the inlet valves. The piston goes up and due to the high compression of the air the temperature rises to over 1000 K. At the end of the stroke, the diesel fuel is injected and self-ignites due to the high temperature.

In the second stroke the piston is accelerated downwards due to the high pressure created by the combustion. All valves are initially closed, but in the end the exhaust valves are opened.

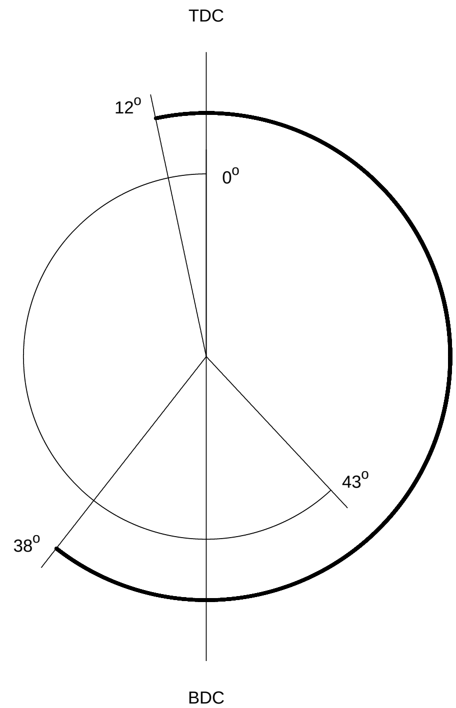

Figure 2.1 *The timings of the valves. The thick circle segment represents the time that the inlet valves are open and the thin represents the time the exhaust valves are open. Begin in BDC and follow the figure two revolutions clockwise. After 38° the inlet valves close and the pressure rises as the piston goes up. Shortly before TDC the diesel usually is injected and after TDC the high pressure presses the piston down again. 43° before BDC the exhaust valves open and the exhaust gases leave the engine when the piston once more goes up. 12° before TDC the inlet valves open to enable the turbo to press the remaining exhaust gases out of the cylinder. After TDC only the inlet valves are open and the cylinder is filled with fresh cold air.*

In the third stroke the piston goes up again. This time the exhaust valves stay open, so the burned gases are pushed out of the cylinder. In the end the inlet valves are opened and the turbo charged inlet air forces the last exhaust gases to leave the engine.

The fourth stroke begins with the closing of the exhaust valves. The cylinder is now filled with fresh, cold air as the piston goes down. After two revolutions of the crankshaft the work cycle is complete and it is time for the first stroke again [5]. The exact timings of the valves can be seen in Figure 2.1.

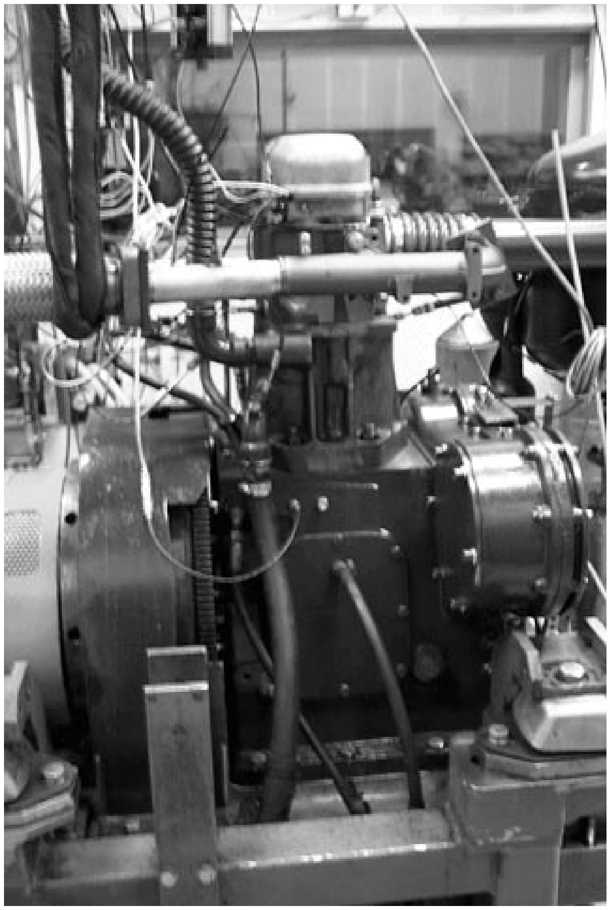

Figure 2.2 *The one cylinder test engine.*

One Cylinder Test Engine

In order to isolate the behavior of one cylinder and enable optimization of the combustion process, one cylinder test engines are used. The engines are identical to full scale engines but has only one cylinder and are developed for experimental purposes only. Because of the simplicity of the engine, the knock signal should be easy to evaluate and this is the reason the engine is used in the experiments. A picture of such an engine can be seen in Figure 2.2.

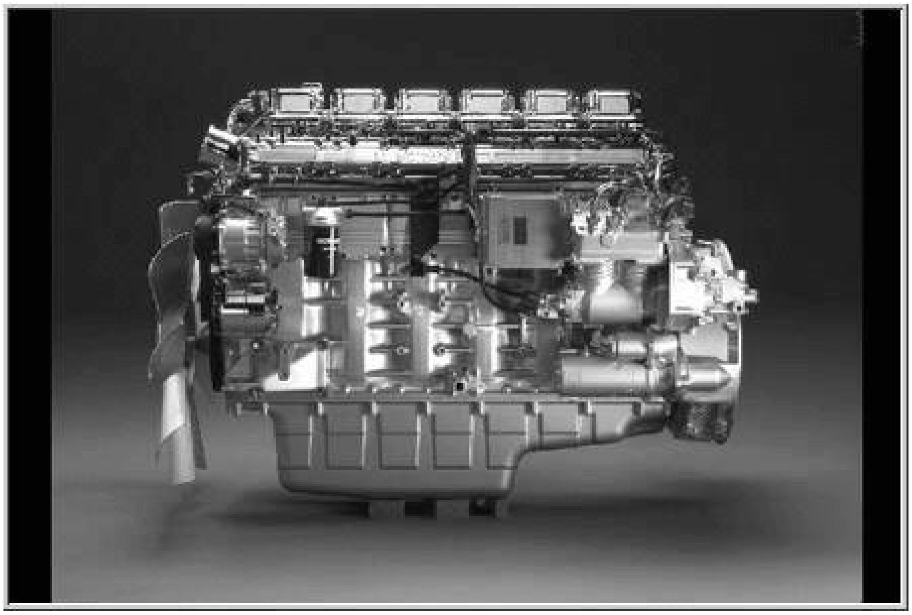

Figure 2.3 *The Scania DC12-01.*

Scania Inline-Six DC12-01 Engine

In a full scale production engine the output of the knock signal is much more complex since all cylinders contribute to the acceleration of the block. In order to test the idea in a more realistic situation an inline-six engine with the following data is used:

Weight:	1180 kg
Max power (1900 rev):	420 HP
Max torque (1100 - 1300 rev):	2000 Nm
Bore:	127 mm
Stroke:	154 mm
Compression ratio:	18:1
Firing order of the cylinders:	1-5-3-6-2-4

This is a typical engine for European long-haulage traffic. Since all cylinders gets their inlet air from left side, this side is cold and therefore called the cold side. The turbo is located on the other side where the exhaust gases leave the engine and this side is very warm and therefore called the warm side. A picture of the engine from the cold side can be seen in Figure 2.3.

Figure 2.4 *From the left: coin, Kistler 7061, Lamerholm VP50/1 and Brüel & Kjær 4393.*

2.2 Sensors

Three types of sensors are used. They are described in the following and shown in Figure 2.4.

Pressure Sensor

The Kistler 7061B is a water-cooled piezo electric pressure sensor.

Knock Sensors

The Lamerholm VP50/1 is a standard knock sensor widely used in the automotive industry. The manufacturer specifies the response band to 2 kHz to 20 kHz.
The Brüel & Kjær 4393 is a high performance piezo electric accelerometer with a response band of 0 to 30 kHz.

Location of the Brüel & Kjær 4393 on the One Cylinder Test Engine

Only one location is used. This is near the top of the engine block. The mounted sensor can be seen in Figure 2.2.

Locations of the Knock Sensors on the DC12-01

Several locations are tried and it is possible to separate them in three different groups.

A - locations on the warm side near the top of the block in order to get measurements from a place near the combustion. Both sensors are used in these experiments. See Figure 2.5 for examples of the locations.

B - a location on the cold side lower on the block. The Lamerholm VP50/1 is used. The exact position can be seen in Figure 2.6.

C - a location on the warm side lower on the block. The Lamerholm VP50/1 is used. The exact position can be seen in Figure 2.7.

The sensors are in all locations mounted to measure horizontal accelerations.

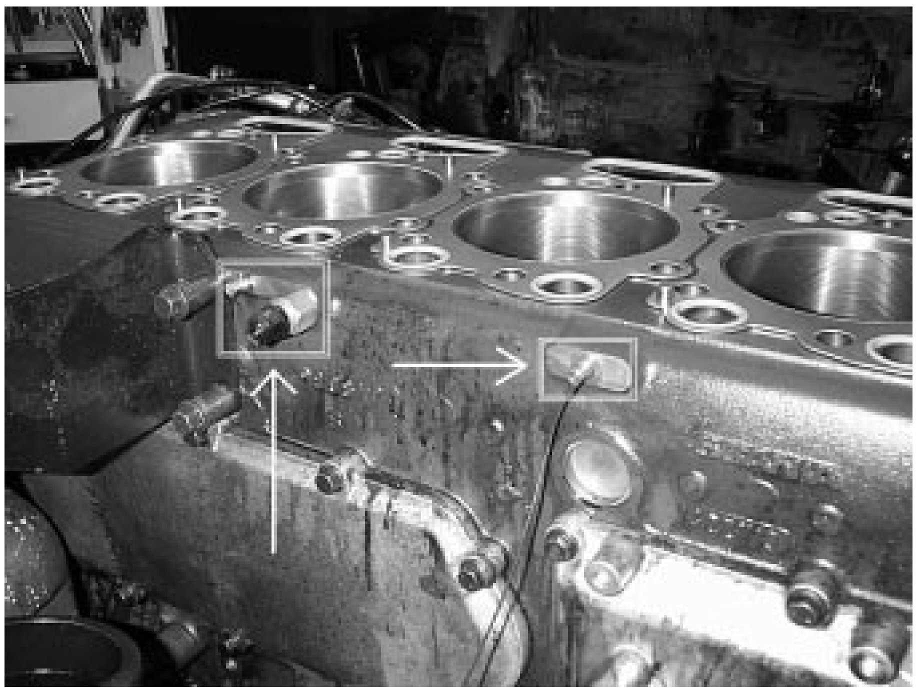

Figure 2.5 *The picture shows a part of the warm side on a Scania DC12-01. The cylinder heads are removed and three sensor locations on the warm side can be seen. A Brüel & Kjær 4393 and a Lamerholm VP50/1 can be seen in the left marking and in the right a Brüel & Kjær 4393 with a connecting cable.*

Figure 2.6 *The picture shows a part of the cold side on a Scania DC12-01. The sensor location named B is marked.*

2.3 Data Acquisition System

An AVL IndiMaster 670 is used as data acquisition system. The instrument is able to sample four channels with 14 bits resolution and eight channels with 12 bits resolution at a maximum frequency of 1 MHz.

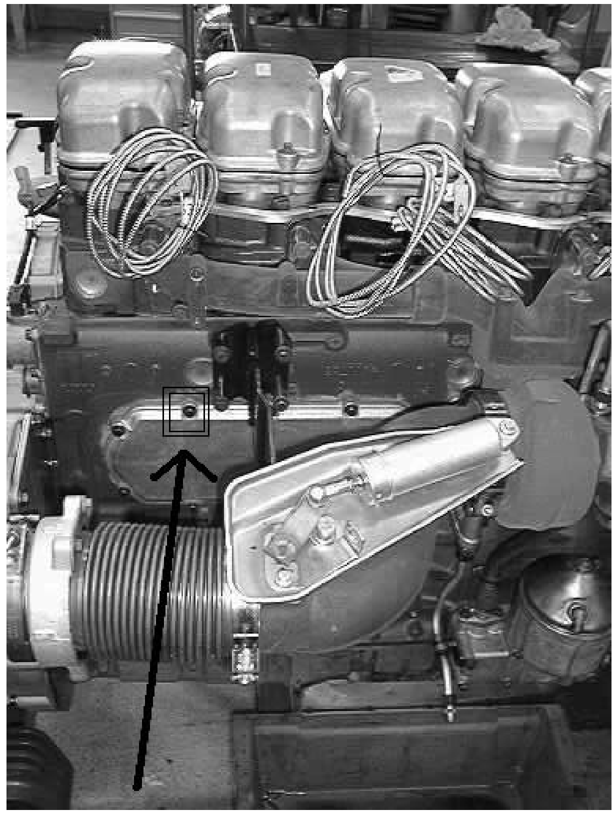

Figure 2.7 *The picture shows a part of the warm side on a Scania DC12-01. The sensor location named C is marked.*

Chapter 3

Experiments

This chapter describes the experiments done and the measured signals. It also contains example plots of unfiltered data.

3.1 Measured Signals

Five different kinds of signals are measured at a sample frequency of 200 kHz. The high frequency is chosen to avoid aliasing and to enable studies of the signals in a wide frequency spectrum.

Cylinder Pressure

This signal is measured with a resolution of 12 bits to enable visible correlation of the detected and the actual SOC. In the cylinder head a channel is drilled. The channel begins in the wall on the warm side of the engine and ends in the combustion chamber. The Kistler 7061B is mounted in the outside end of the channel.

Needle Lift (SOI)

The signal describes the position of the needle mentioned in Section 2.1. The signal is typically zero but for times of injections when it forms a pulse of varying length but of fixed amplitude. SOI is defined to occur at the point of time when the needle has moved a third of its way, i.e. the pulse has reached a third of its amplitude. The used resolution is 12 bits.

Crank Angle Information

A plate with 1800 radial lines is mounted to the crankshaft. An optical sensor sends pulses for every line that passes it. This leads to a signal that consists of five pulses every angle the crank rotates.

Trig Signal

There is one more line on the plate mounted to the crankshaft. By measuring the position of this line and counting the pulses from the crank angle information, it is possible to calculate the momentary crank angle with an accuracy of 0.2 degrees. The used resolution is 12 bits.

Knock Signals

The signal measures how the block accelerates and is, along with the crank angle, used as input in the SOC calculations. To enable as exact measurements as possible, the signal is measured with a resolution of 14 bits. Because of the high frequency noise in the signal, it is low pass filtered before it is sampled. The chosen cut of frequency is 30 kHz, because of a resonance frequency especially in the Brüel & Kjær 4393 sensor.

3.2 One Cylinder Test Engine Experiment

The main reason for the one cylinder test engine series is to get a simple system in which there is as little unpredictable noise as possible. Thirteen experiments have been made in three subseries and the Brüel & Kjær 4393 is used in all of them. Example data can be found in Figure 3.1.

One Cylinder Subseries 1

Experiment no.	EGR	r.p.m.	load	α
1	20 %	1400	100 %	-3
2	14 %	1400	100 %	-3
3	10 %	1400	100 %	-3
4	5 %	1400	100 %	-3
5	–	1400	0 %	–

One Cylinder Subseries 2

Experiment no.	EGR	r.p.m.	load	α
6	0 %	1800	50 %	-9
7	0 %	1800	50 %	-5
8	0 %	1800	50 %	-1
9	0 %	1800	50 %	3

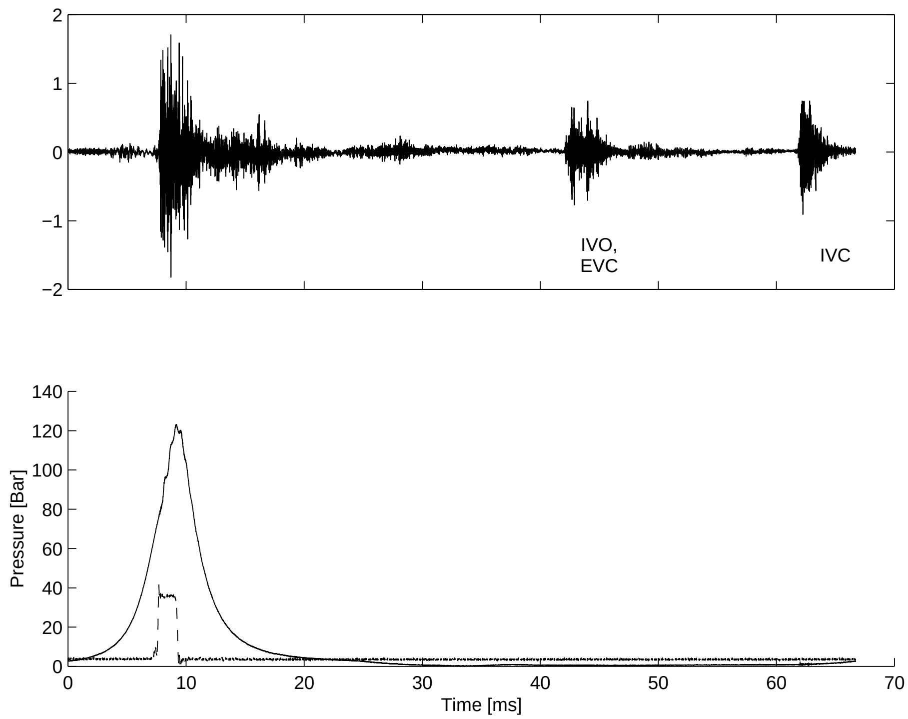

Figure 3.1 *Data from four strokes in the one cylinder test engine experiment. The upper graph shows the knock signal and the lower the pressure (solid) and the injection (dashed). Around 8 ms it is possible to see the combustion in the knock signal, between 40 ms and 50 ms the inlet valves open (IVO) and the exhaust valves close (EVC) and finally the inlet valves close (IVC) after 60 ms.*

One Cylinder Subseries 3

Experiment no.	EGR	r.p.m.	load	α
10	–	1200	0 %	–
11	0 %	1200	50 %	-6
12	0 %	1200	100 %	-6
13	20 %	1200	100 %	-3

3.3 DC12-01 Experiment

Twelve experiments has been made in two subseries with six experiments in each. The two subseries are identical except for the location of the knock sensor. In the first subseries the sensor location B is used and in the second location C. In both

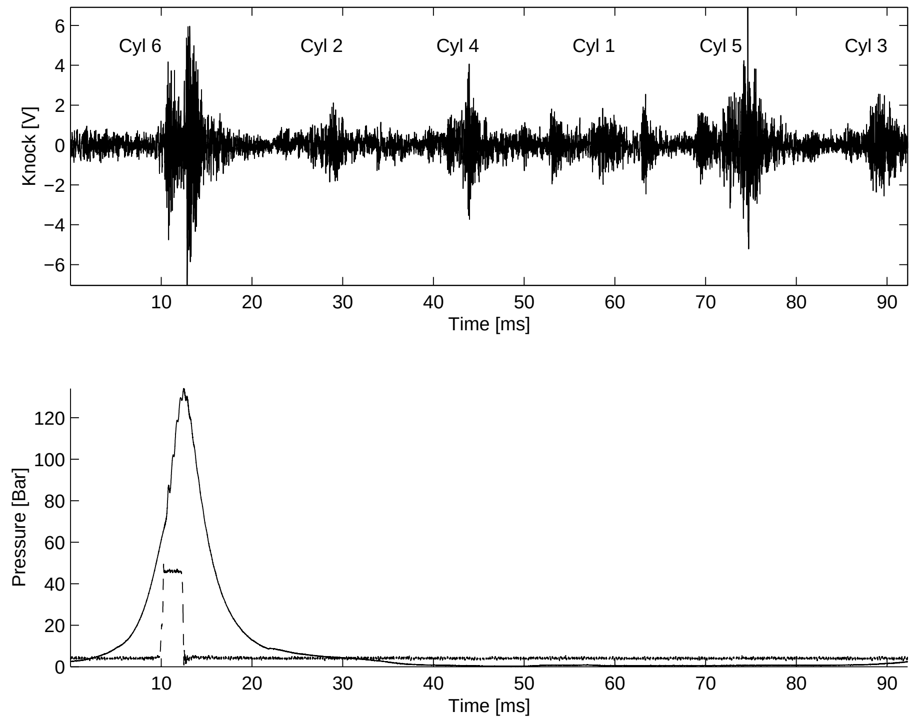

Figure 3.2 *Data from four strokes in the DC12-01-experiment. The upper graph shows the knock signal and the lower the pressure and the injection. Compared to Figure 3.1 it is here much more complicated to correlate the knock with events because of the complexity of the engine.*

subseries the VP50/1 has been used. Example data can be seen in Figure 3.2.

DC12-01 Subseries 1 and 2

Experiment no.	EGR	r.p.m.	load	α
14, 20	0 %	1300	50 %	-12
15, 21	0 %	1300	50 %	-9
16, 22	0 %	1300	50 %	-6
17, 23	0 %	1300	50 %	-3
18, 24	0 %	1300	50 %	0
19, 25	–	1300	0 %	–

Chapter 4
SOC Detection Algorithm

The objective of this chapter is to explain the chosen strategy for SOC detection. It begins by explaining the similarities in the knock detection in SI engines and the SOC detection problem in diesel engines. The chosen method is then presented. The second last section of the chapter discusses two different pressure based methods to find SOC and the last the rather important question *"What have we detected?"*.

4.1 Background

In SI engines knock is the problem of auto ignited fuel which must be detected. Several algorithms are developed to make this detection possible [7]. The algorithms present a "yes" or "no" answer. Steps are thereafter taken to avoid knock in the next cycle. This study however aims at the development of an algorithm that detects the very instant SOC occurs.

From studies on SI engines, it is known that the knock frequencies are fairly independent of the ratio of compression and the engine speed. The resonance frequencies f_k can be calculated with Equation 4.1,

$$f_k = \rho_{mn} \frac{c}{\pi B} \tag{4.1}$$

where ρ_{mn} is the mode constant, c the sound velocity and B the bore. The different modes are different stationary wave systems [7]. The sound velocity can be calculated with Equation 4.2,

$$c = \sqrt{\kappa R T} \tag{4.2}$$

where κ is the isentropic exponent and equals 1.4, R the gas constant and equals 287 and T the average gas temperature in the cylinder [4]. The bore in the DC12-01 is 127 mm and the temperature during the early combustion is approximately 1200 K. It is now easy to calculate the speed of sound to 630 m/s and to get Table 4.1.

ρ_{mn}	f_k
1.841	3.2 kHz
3.054	5.3 kHz
3.832	6.7 kHz
4.201	7.3 kHz
5.332	9.3 kHz

Table 4.1 *The different mode constants and their correlating knock frequencies.*

Now that these frequencies of the knock are known, it should be an easy task to maximize the signal to noise ratio (SNR) by applying a filter with pass band at one of the knock frequencies. In order to get a detection feasible in real time, the filter should not work on data from the entire cycle, but on short intervals around the expected SOC. This not only shortens the time needed for the calculations but also simplifies the calculations because uninteresting intervals are avoided.

4.2 Filter

The Matlab Signal Processing Toolbox includes the *specgram* command that produces time-frequency diagrams by making many FFTs of the same length. The amplitude of the FFTs is thereafter translated to colors and presented in vertical lines and the diagrams can be seen as colorful pictures [6]. These pictures were found very useful in the choosing of a filter pass band. By using time-frequency techniques as shown in Figure 4.1 the pressure, SOI and amplitude of the knock at different frequencies can simultaneously be studied. A ripple can be found in the pressure at approximately 1.5 ms. This can be seen at all loads and speeds and occurs a short time after SOI and a detection that coincide with that is taken as a detection of the start of the combustion. A study of Figure 4.1 shows that a very distinct shift in the amplitude (color) of the knock in the 20 - 30 kHz band appears at that time. This is very repeatable from cycle to cycle and therefore the chosen pass band of the filter is, somewhat surprisingly considering the SI results, chosen to 20 - 30 kHz.

Because of the Kistler 7061B location in a channel (See Section 3.1), a standing wave that begins shortly after the ripple begins can be found in the pressure signal. It is possible to calculate the frequency f of the wave with Equation 4.3,

$$f = \frac{c}{4r} \tag{4.3}$$

where c still is the speed of sound and r is the length of the channel [4]. Since r is 7 cm, f can theoretically be found to be 2480 Hz. From the figure an experimental value can be calculated. This is 2.5 kHz.
In figure 4.2 the reader can compare the knock with the filtered knock, the pressure

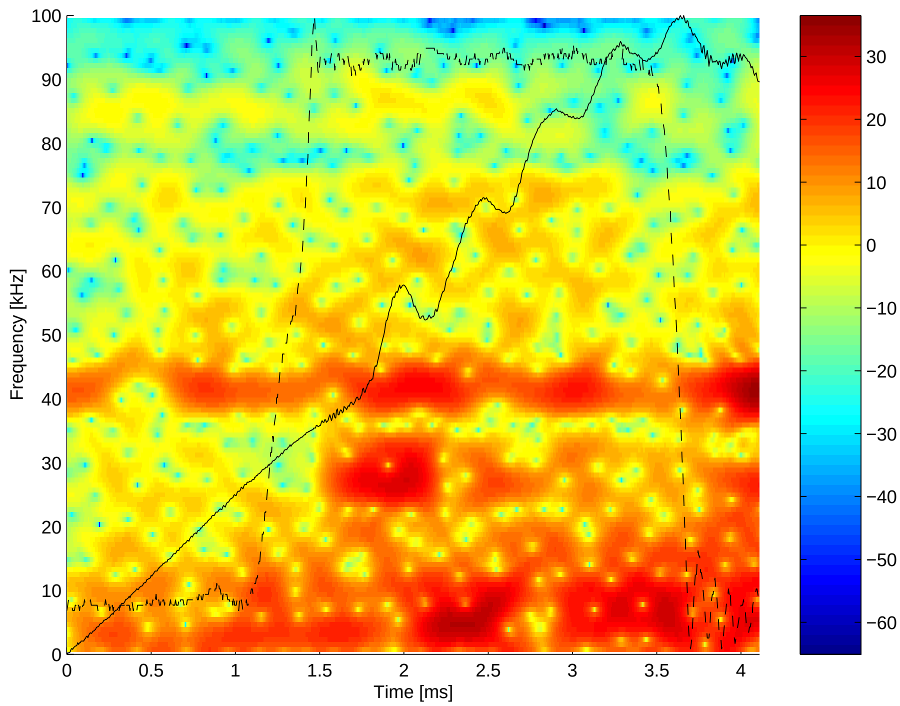

Figure 4.1 *Time-frequency study of the knock. The momentary frequency content of the unfiltered knock can be studied by comparing the colors on imagined vertical lines. The amplitude of the spectrum can be seen in the color bar to the right. The cylinder pressure (solid) and the injection information (dashed) is plotted to simplify the interpretation of the figure. A ripple in the measured pressure can be seen at approximately 1.5 ms. At the same time the knock signal starts to contain energy in the 20 kHz to 30 kHz band. This is very typical and repeatable. Note also the standing wave phenomenon in the pressure from 1.8 ms. This might arise from the channel the Kistler 7061B is mounted in.*

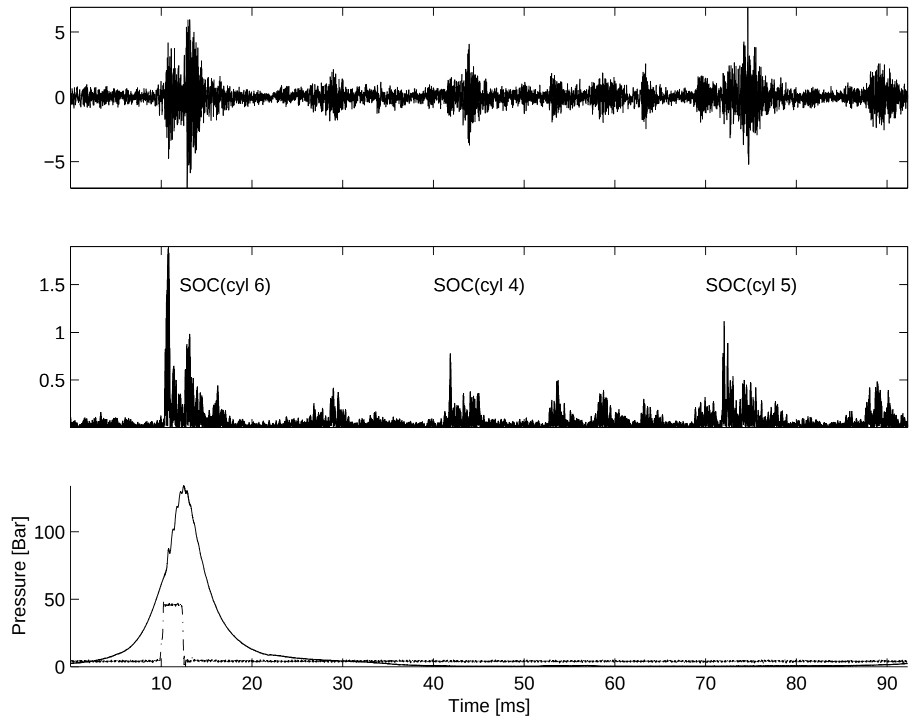

Figure 4.2 *At the top the unfiltered knock is shown, in the middle the filtered knock and at the bottom the pressure of cylinder six and the SOI-indication. The knock intensity for cylinder four, five and six is larger because the sensor is closer to them.*

and the SOI-indicator.

4.3 Envelope

A signal sampled with a fixed frequency can look very different due to the start of the sampling. Take for example the signal in Figure 4.3. It is generated with the function from Equation 4.4.

$$f = \frac{(1 - \cos(4\pi t))\sin(64\pi t)}{2} \tag{4.4}$$

In Figure 4.4 the same signal is sampled much slower and two different starting times is used. It is hard to see that the two curves come from the same original curve. From these plots it is clear that it would be much more interesting to know the envelopes, i.e. momentary energies, of the knock signal than the momentary

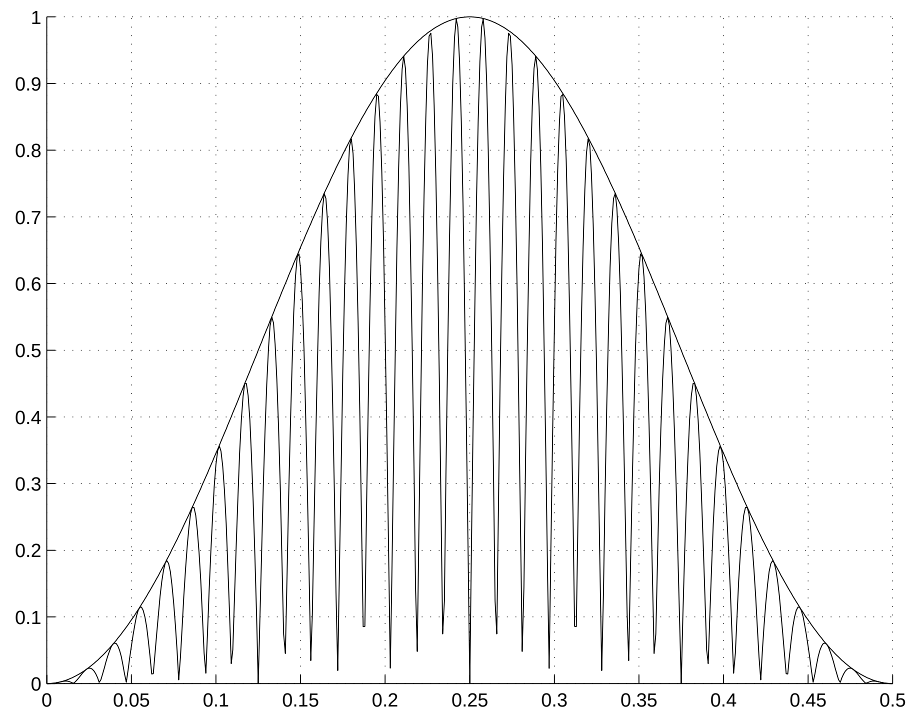

Figure 4.3 *The signal from Equation 4.4 is shown along with its envelope.*

value. That they resemble each other and the original envelope better than the curves individual do is clearly seen. The envelopes are calculated by low pass filtering the absolute value of the filtered signals. This may seem strange when the signals already are band pass filtered, but by the absolute value operation, we get completely new signals. The cut off frequency is taken as half the lower cut off frequency of the first filter, i.e. 10 kHz. In Figure 4.5 a band pass filtered signal can be seen with its envelope.

If the detection is said to be achieved when the momentary energy exceedes a given threshold, it is better to use the envelope of a signal then the signal itself. This can be seen in Figure 4.4. The dashed curve exceeds the threshold two samples earlier than the solid, but the envelopes exceed it at the same time.

4.4 Threshold

A rather simple method of detecting the combustion is now used. When the envelope of the filtered signal exceeds a given threshold, the combustion is said to have started. The level should be set as low as possible to have a fast detection,

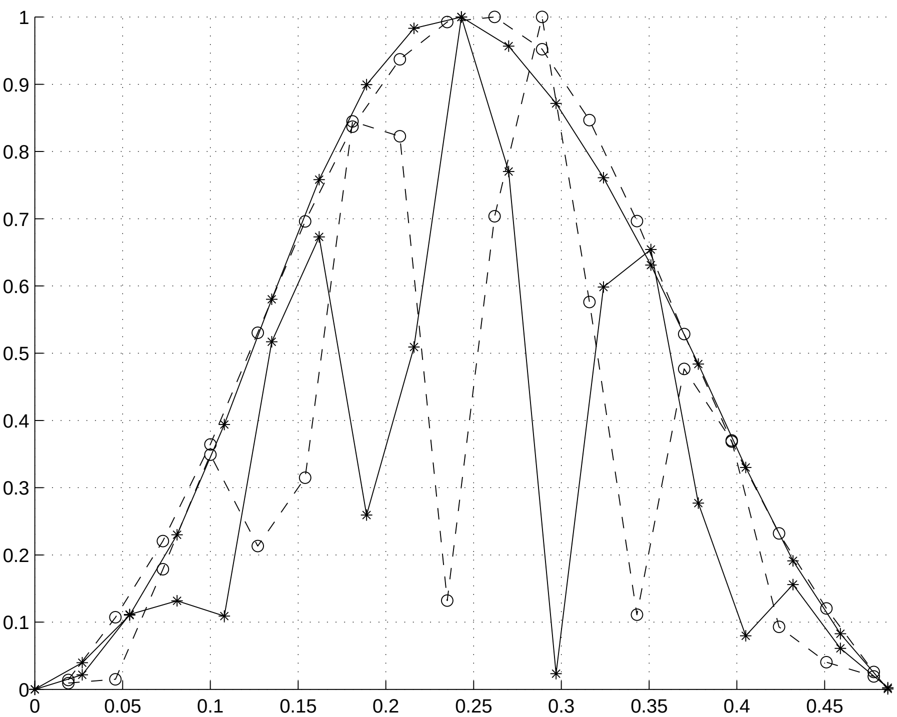

Figure 4.4 *The signal from Equation 4.4 is here sampled 27 times slower and with two different offsets in the starting time. Note first how different the curves are and then how similar the envelopes are to each others and to the envelope in Figure 4.3!*

but higher than the unseparable noise. In Figure 4.5 the important local minimum problem is seen. The shape of the envelope differs slightly from cycle to cycle and an ill-considered threshold could randomly hit the envelope before or after the minimum. Empirical experiments shows that 30 % of the maximum of the envelope is a suitable level. The threshold is expressed in percentages to make sure that the same threshold works for different speeds, loads and amplifications as well as for different cylinders and even different sensors.

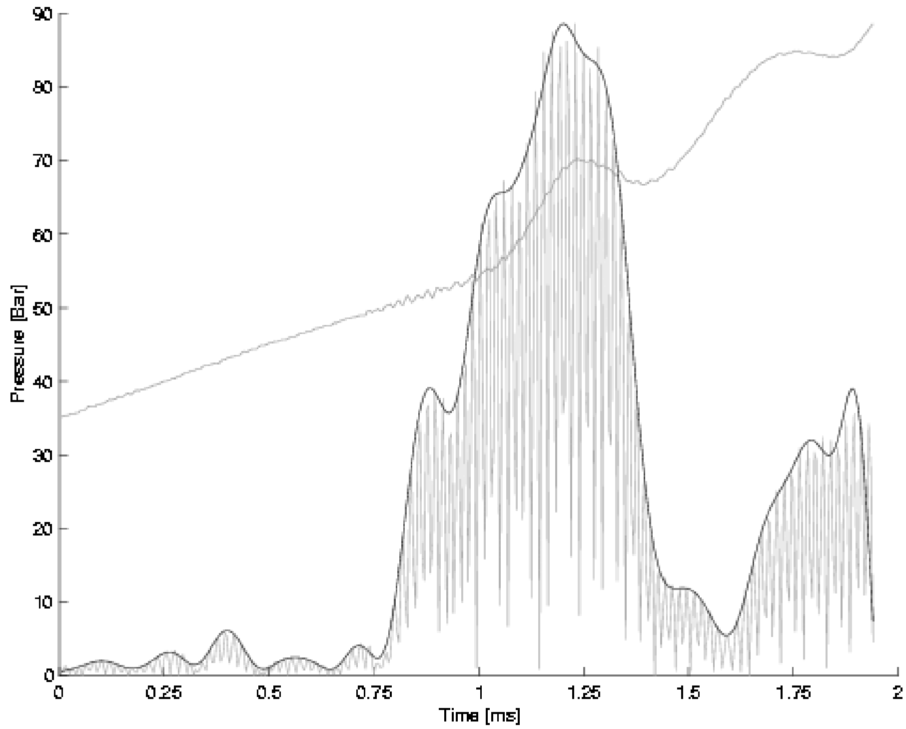

Figure 4.5 *The picture shows a typical pressure, absolute value of the filtered knock and envelope of the filtered knock (both rescaled to fit better in the plot). Note the local minimum of the signal between 0.75 ms and 1 ms. To minimize the cycle to cycle variation of the detection, it is important to set the threshold below this amplitude of the envelope. Note also the ripple in the pressure during the same time.*

4.5 Pressure Correlation

The aim of this study is to enable closed loop control strategy of SOC. The important issue is not to find the actual SOC, but a combustion timing that is robust and repeatable at all speed and loads. The goal is to eliminate the component to component variations in the diesel injection system and to maintain the performance of the engine. A way to prove the validity of the estimation, the knock detected SOC (SOC_k) can be compared to SOC determined from the cylinder pressure. Two ways to do that are presented here.

Heat Release

One such way is the heat release strategy. This method compares cylinder pressure in a combustion cycle to the theoretically calculated pressure in a non-combustion cycle and through that enables us to calculate the momentarily temperature and energy extracted from the combustion [2, 5]. Figure 4.6 shows an example of data calculated with the technique and explains it further. This method is not investigated in this report.

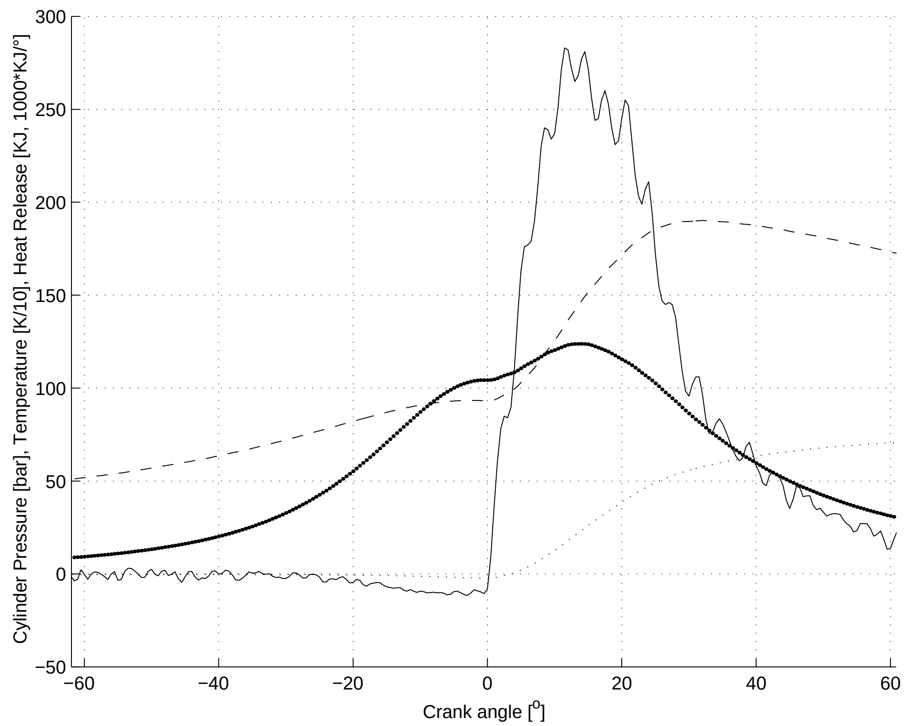

Figure 4.6 *Heat release data from an inline-six engine. The cylinder pressure is bold, the temperature dashed, the heat release solid and the integrated heat release dotted. The heat release curve shows the energy the diesel releases. Due to the energy loss as the diesel vaporizes, the curve has negative sign before* $\alpha = 0$*. SOC is defined as the instant when the heat release curve exceeds zero.*

Pressure Ripple

Another way is to evaluate the pressure ripple with a method similar to the one used when evaluating the knock signal. The ripple is interpreted as the early combustion. The resulting envelope of the band pass filtered pressure can be seen in

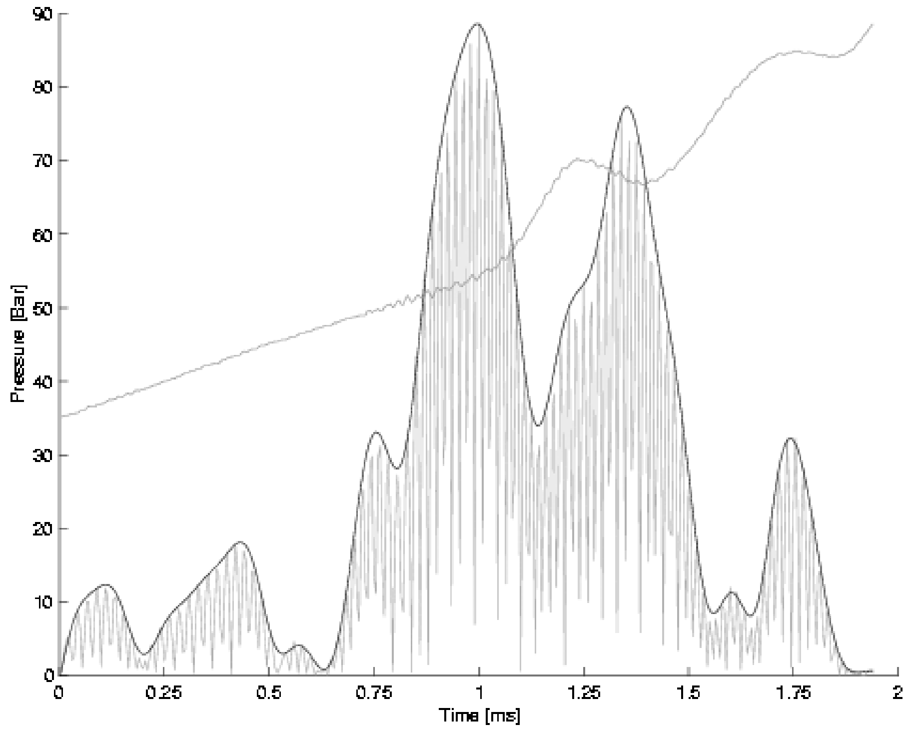

Figure 4.7 *The pressure, the filtered pressure and the envelope of the filtered pressure are shown. Two major differences from Figure 4.5 are the relative high level of the signal before SOC and the less stable local minimum at 0.8 ms. These complicate the detection.*

Figure 4.7. By choosing the threshold 35 %, it is possible to get a detection, but the ripple detected SOC (SOC_p) is not as stable as SOC_k. This is because of the difficulties in choosing a good threshold. The difference between the pressure ripple envelope in consecutive combustions is bigger than that of the knock. SOC_p however is a way to, at least roughly, quantify the visible ripple.

4.6 SOI or SOC Detection?

Since the injectors used in the experiments include moving details, the ripple in the pressure and the measured knock *could* originate from SOI instead of SOC. To ensure us that this is not the case, the delay between SOI and SOC_k as well as the delay between SOI and SOC_p are shown in Figure 4.8. If the detections were SOI detections, they would appear a fix period after SOI independent of the

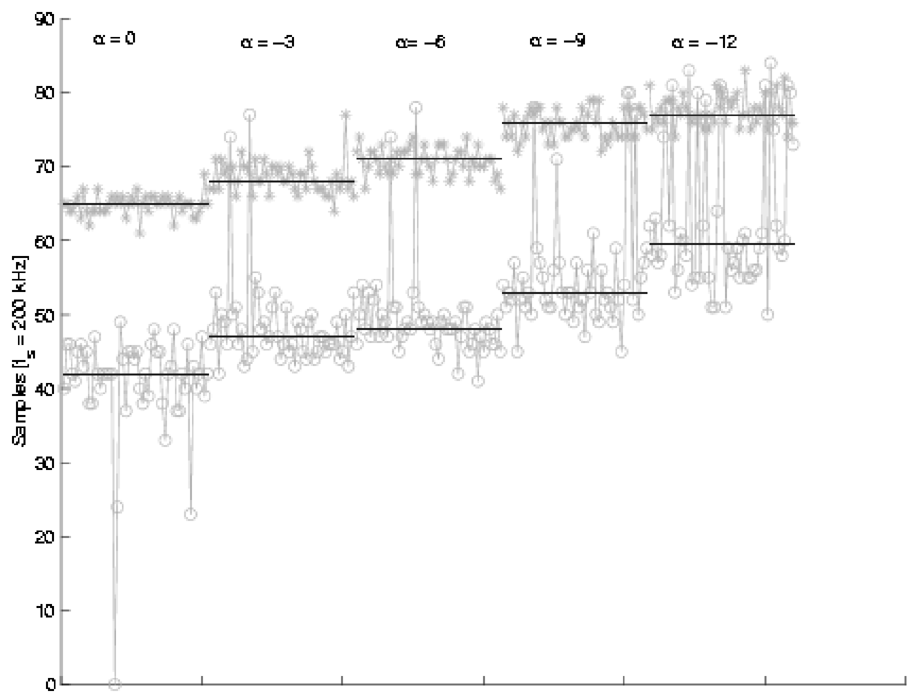

Figure 4.8 *Here are all combustions from the DC12-01 experiments shown. The circles represent the delays from SOI to SOC_p, the asterisks the delays from SOI to SOC_k and the horizontal lines are the medians in the different experiments. Even if the detections are rather noisy, the trend of longer delays can be seen in both detections. The experiment are shown with no 20 from the left and then 21, 22, 23, 24.*

injection timing, *but this is not the case*. Both detections appear later and later if the injection begins earlier and earlier. Since the rise in the temperature in the cylinder originates from the rise in the pressure, an early injection means that the temperature in the cylinder is lower. This means reasonably that the delay should be longer. It is easy to see that SOC_p is not as stable as SOC_k. The really early detections of SOC_p depends on the high magnitude noise before the interesting time window.

Chapter 5
Results

This chapter presents the chosen locations of the sensors as well as the statistical results from the detections.

5.1 Knock Sensor Locations

The DC12-01 experiments show that the sensor locations are very important. Figure 5.1 illustrates the problems with sensor location A. The injection of one cylinder is here suddenly turned off and the last engine cycle with fuel is seen together with the first without. After a study of figure 2.1 it can be concluded that the valves of other cylinders are big sources of noise. Figure 5.2 is helpful when analyzing the influence. Of crucial importance in the time-window-strategy used is that the noise in the window must be filtered away. The valves however cause a kind of noise that is indistinguishable from the combustion knock. In sensor locations B and C however, the noise originating from the valves is less intense because of the fact that the locations are farther away from the valves. As will be seen in Table 5.2, the standard deviation of the SOI-SOC_k delay is lower in experiments with the knock sensor in location C, so that location is chosen.

5.2 SOC Detection Results

By mounting the knock sensors according to section 2.2 and using the filter from section 4.2, a steady detection of SOC was received. The reliability can be measured in view of two quantities: standard deviation and visual correlation.

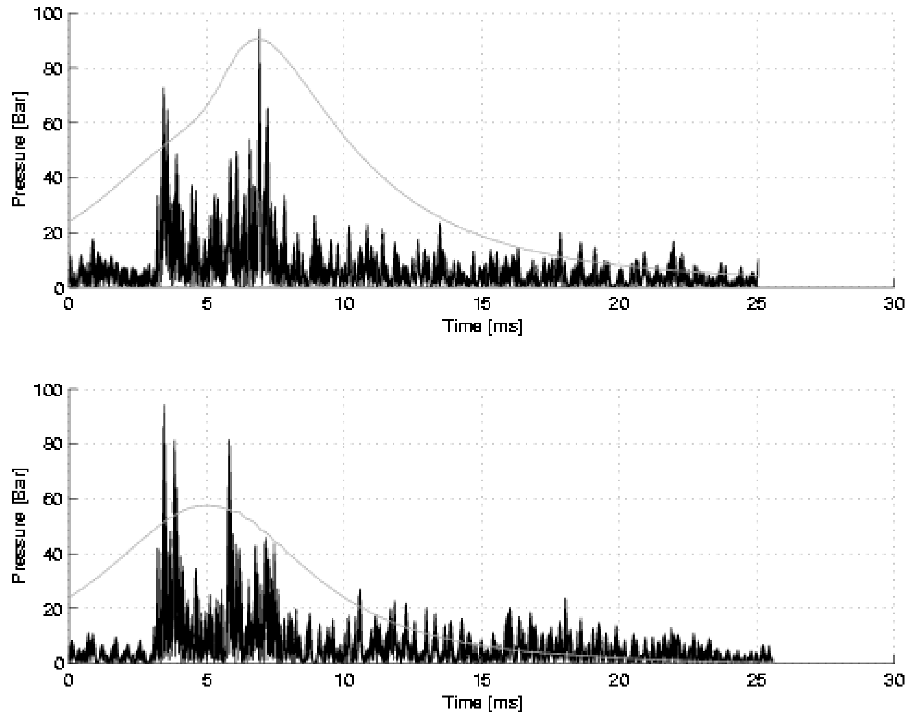

Figure 5.1 *The pressure in cylinder five and the filtered knock measured in two consecutive cycles. The knock sensor is mounted in location A. Note that the beginning of the knock hardly at all differs, although there is no combustion in the second figure.*

Statistical Standard Deviations

The standard deviation of the detection is calculated along with other quantities over fifty consecutive engine cycles. Table 5.1 presents the results from the one cylinder tests without EGR. In a random number of the cycles in every one cylinder test engine experiments a fix offset is added. Now the standard deviations of SOI and SOC_k will be big, but if the detection works, the SOI-SOC_k delay will be significantly smaller. As an example the pressure, measured SOI and SOC_k for all cycles in experiment 11 can be seen in Figure 5.3. The smallest standard deviation, often by far, is the SOI-SOC_k delay standard deviation. This means that SOC_k varies along with SOI.

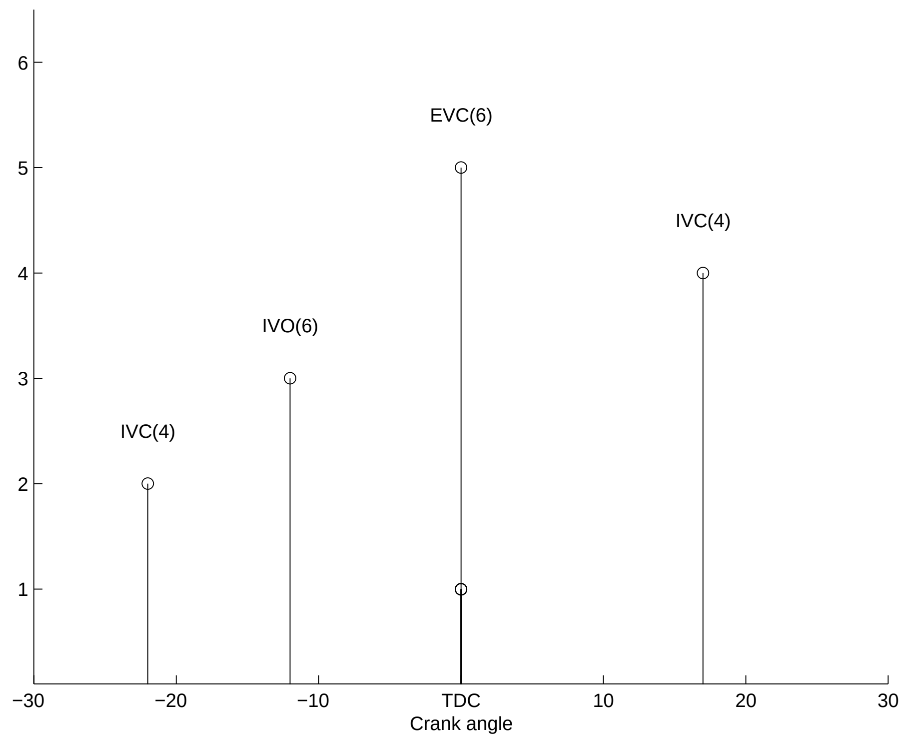

Figure 5.2 *The different events around TDC of cylinder one in the Scania DC12-01 engine. At -22 the inlet valves of cylinder four closes. At -12 the inlet valves of cylinder six opens. At TDC the exhaust valves of cylinder six closes. At 17 the exhaust valves of cylinder 5 opens. Similar schedules can be drawn for all cylinders.*

	SOI		SOC_p		SOC_k		SOI - SOC_k		SOI - SOC_p	
Exp no	Mean	Std	Mean	Std	Mean	Std	Mean	Std	Mean	Std
6	-8.94	0.25	-8.10	0.32	-7.00	0.25	1.94	0.08	1.10	0.18
7	-4.95	0.31	-4.20	0.49	-3.09	0.32	1.86	0.10	1.11	0.36
8	-0.55	0.38	0.37	0.42	1.16	0.41	1.71	0.09	0.79	0.20
9	2.63	0.31	5.29	0.32	6.20	0.26	3.57	0.10	0.91	0.10
11	-5.76	0.16	-4.39	0.29	-3.54	0.17	2.22	0.05	0.85	0.19
12	-6.02	0.07	-4.74	0.34	-3.69	0.08	2.33	0.05	1.05	0.33

Table 5.1 *Statistics from the one cylinder experiments over 50 cycles. Compare the SOI - SOC_k columns with the SOI columns. The SOI - SOC_k standard deviations are clearly smaller than the SOI standard deviations.*

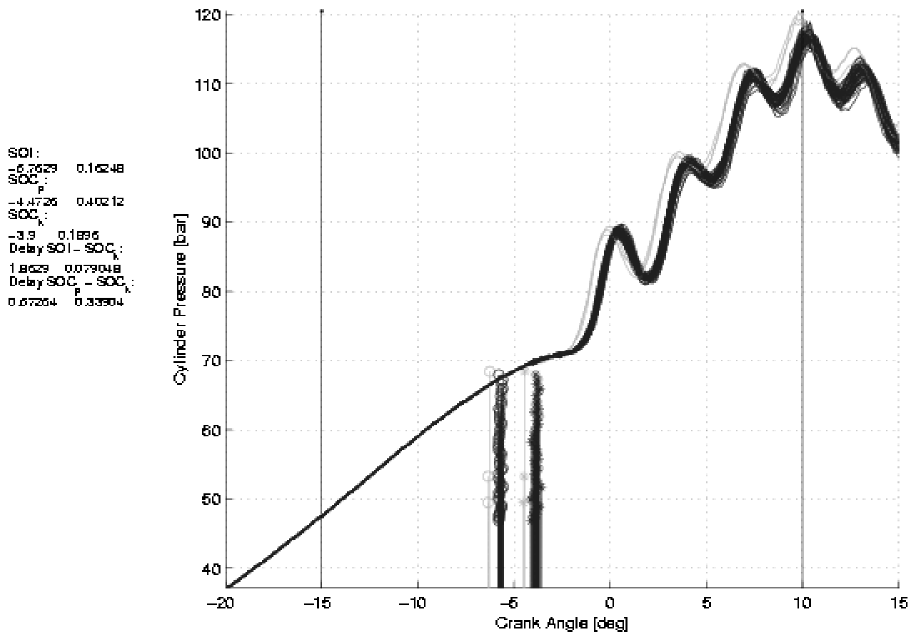

Figure 5.3 *All cycle results from experiment no 11 are shown. The correlating pressure, SOI (circles) and SOC_k (asterisks) are plotted in the same color. The early detections are plotted grey. Note that SOI and the rise of the pressure waves of early SOC_k is earlier than those of the late SOC_k! To the left some statistics can be seen.*

Visual Correlation of the Ripple and SOC_k

To enable visual correlation of the ripple mentioned in Section 4.2, six pressure waves from different engine cycles are shown in Figure 5.4. Figure 5.5 shows the same traces but in detail. Here it is clear that SOC_k and the occurrence of the ripple correlate.

5.3 Statistics From Scania DC12-01

The cycle to cycle SOC detection reliability can be seen in Table 5.2. The knock sensor location used is location B and C and it is here clear that location C is to prefer. It is also clear that the standard deviation of the SOI-SOC_k delay is of approximately the same magnitude that the SOI standard deviation. Section 4.5 explains SOC_p and why it is rather unreliable, but in Figure 4.8 it is clear that a median value of several cycles could be a good measure. It is also clear that the ignition delay changes with the injection angle. This is quite logic due to the

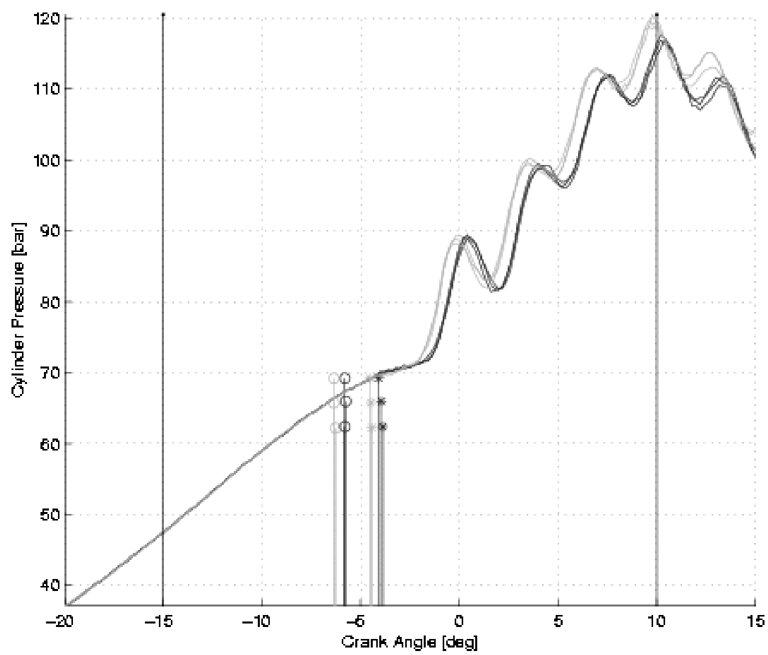

Figure 5.4 *Results from experiment no 11. Six pressure waves on top of each other are shown together with the measured SOI (circles) and SOC_k (asterisks) for each cycle. The stems of the same height correlate with each other and with pressure waves of the same color. Early detections are plotted grey. It is obvious that early detections correlate with pressure waves with early rise in the pressure.*

different compression of the air in the cylinder. Higher compression results in higher temperature and this should logically lead to shorter delay.

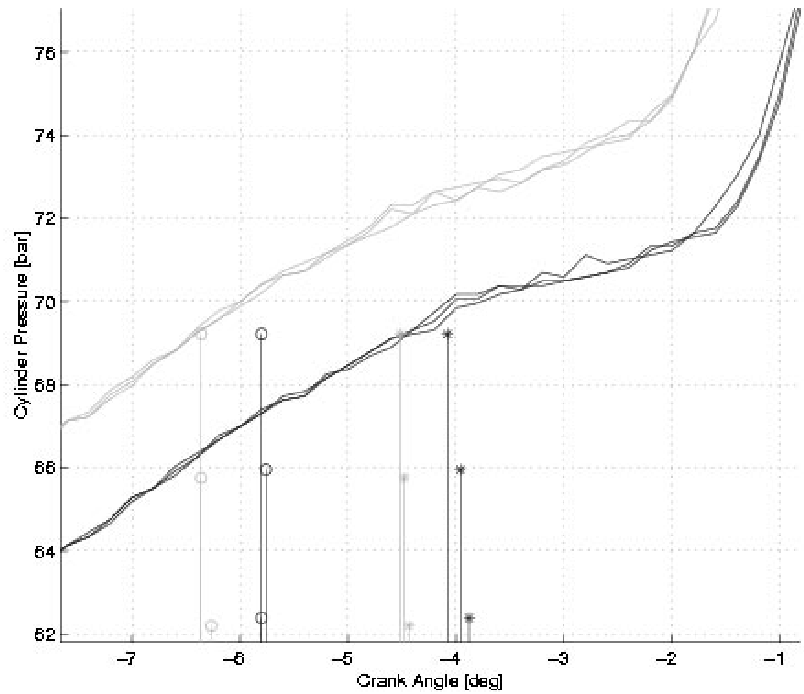

Figure 5.5 *The same data as in Figure 5.4 but enlarged. An offset is added to the pressure waves of the early detections are to make it easier to see the ripple in the pressure that in the grey curves appear approximately 0.5 degree earlier than in the dark curves, i.e. the pressure waves of that correlate with the late detections.*

	Sensor	SOI		SOC_p		SOC_k		SOI - SOC_k		SOI - SOC_p	
Exp no	location	Mean	Std	Mean	Std	Mean	Std	Mean	Std	Mean	Std
24	C	0.10	0.08	1.71	0.29	2.62	0.10	2.52	0.05	0.91	0.31
18	B	0.28	0.11	1.87	0.36	3.44	3.06	3.16	3.06	1.57	3.12
23	C	-2.95	0.04	-1.07	0.24	-0.29	0.09	2.67	0.08	0.78	0.24
17	B	-2.89	0.05	-1.20	0.50	0.65	1.90	3.54	1.89	1.85	2.00
22	C	-5.93	0.04	-4.00	0.23	-3.16	0.08	2.78	0.07	0.85	0.24
16	B	-5.84	0.04	-3.87	0.27	-1.77	0.26	4.06	0.26	2.10	0.35
21	C	-8.99	0.07	-6.84	0.33	-6.04	0.09	2.95	0.07	0.79	0.31
15	B	-8.94	0.06	-6.82	0.19	-4.63	0.13	4.31	0.12	2.19	0.20
20	C	-11.91	0.16	-9.46	0.39	-8.92	0.13	2.99	0.08	0.54	0.39
14	B	-11.97	0.15	-9.74	0.30	-7.58	0.25	4.40	0.25	2.16	0.37

Table 5.2 *The table shows statistics from the DC12-01 experiments over 50 cycles. The results are presented by increasing SOI. Experiments no 24, 23, 22, 21 and 20 are sensor location C experiments. In the SOI - SOC_k-columns the differences between the quality of location B and location C can be compared. The standard deviations of the location C experiments are are clearly smaller than those of the sensor location B experiments. Compare also with the SOI standard deviations. The SOI - SOC_k standard deviations are of the same magnitude.*

Chapter 6

Conclusions

The benefits from knowing SOC are many. The ability to optimize the fuel consumption versus the NOx production is one of the more important.

This report describes a method that detects SOC based on knock sensors widely used in the personal car industry. The used idea is to band pass filter a sampled knock signal and thereafter calculate the envelope of the resulting signal. SOC is said to occur when the envelope exceeds 30 % of the maximum amplitude of the envelope. The frequency band chosen for the filter is 20 kHz to 30 kHz, which is surprisingly high compared to SI engine knock algorithms.

It can be concluded from the results that on the Scania DC12-01 the knock signal should be measured from a location on the warm side and approximately one decimeter from the top of the engine block (sensor location C). By using that location and the algorithm from above, the delay between the start of injection and the detected SOC can be calculated with a standard deviation of approximately 0.1 crank angle degree. This can be compared to the standard deviation of the closed loop controlled start of injection (SOI) that is of the same magnitude or only slightly smaller. Because of the accuracy of the algorithm, the detection can be used to control SOC on a cycle to cycle basis.

The overall conclusions is that computer evaluated knock signals offer a cost effective alternative for performing closed loop control of SOC as well as several on board diagnostic features.

Bibliography

[1] Bosch. *Dieseleinspritztechnik im Überblick*, December 1996.

[2] John E. Dec. A conceptual model of DI diesel combustion based on laser-sheet imaging. *SAE 970873*, 1997.

[3] M. Glavmo, P. Spadafora, and R. Bosch. Closed loop start of combustion control utilizing ionization sensing in a diesel engine. *SAE 1999-01-0549*, 1999.

[4] K. Gschweitl, E. Gotthard, and A. Kampitsch. Real time knock analysis for automatic engine mapping and calibration. *SAE 942399*, 1994.

[5] John B. Heywood. *Internal Combustion Engine Fundamentals*. McGraw-Hill Book Company, 1988.

[6] MathWorks. *Signal Processing Toolbox User's Guide*, December 1996.

[7] N. Nakamura, E. Ohno, N. Kanamaru, and T. Funayama. Detection of higher frequency vibration to improve knock controllability. *SAE 871912*, 1987.